

# Quantum Cellular Automata Pseudo-Random Maps

Yaakov S. Weinstein<sup>1,\*</sup> and C. Stephen Hellberg<sup>1,†</sup>

<sup>1</sup>*Center for Computational Materials Science, Naval Research Laboratory, Washington, DC 20375*

Quantum computation based on quantum cellular automata (QCA) can greatly reduce the control and precision necessary for experimental implementations of quantum information processing. A QCA system consists of a few species of qubits in which all qubits of a species evolve in parallel. We show that, in spite of its inherent constraints, a QCA system can be used to study complex quantum dynamics. To this aim, we demonstrate scalable operations on a QCA system that fulfill statistical criteria of randomness and explore which criteria of randomness can be fulfilled by operators from various QCA architectures. Other means of realizing random operators with only a few independent operators are also discussed.

PACS numbers: 03.67.Lx 03.67.Mn

The traditional approach to quantum computation has been through the circuit model: a series of one and two-qubit gates are applied to specified qubits in a specified order [1]. Such an architecture requires exquisite control of each individual qubit and accurate localization of the external Hamiltonian. An alternative approach to quantum computation utilizes quantum cellular automata (QCA). A QCA system consists of just a few (typically 1-3) species of qubits such that all qubits of a species are addressed equivalently and simultaneously.

The idea of using a QCA system for quantum computation was introduced by Lloyd [2] more than a decade ago. Lloyd demonstrated the universality of a three-species QCA and provided pulse sequences for fundamental gates. Further work on QCA has concentrated on proving universality [3], including the universality of a two species QCA that is unable to distinguish the left neighbor from the right [4]. Only recently has there been an attempt to exploit the uniqueness of the QCA architecture to enhance quantum information processing protocols. Brennen and Williams [5] demonstrated the production and manipulation of entanglement in a QCA architecture. In this work we attempt to utilize the QCA architecture in the study of complex quantum dynamics.

Classical cellular automata (CCA) are systems that follow a simple set of local rules applied uniformly to a lattice of cells [6]. Each cell can have an arbitrary number of possible states and, at every time interval, the state of each cell is updated based on its current state and the state of a given radius of nearest neighbors. For example, the evolution of a two-state, radius one, one-dimensional CCA updates cell  $j$  based on its own state and the state of its nearest neighbors. In this case, the evolution has eight update directives, one per combina-

tion of the three two-state cells,  $j - 1$ ,  $j$ , and  $j + 1$ . All cells in a CCA evolve in parallel. This is done by copying the current CCA state for the cells to refer to when updating. Though an apparently simple system, CCA rules can develop complex behavior and can simulate a wide range of phenomena from lattice gases to traffic flow.

A QCA consists of a lattice of quantum cells, each with an arbitrary number of levels. The dynamics of each cell can depend on a given radius of nearest neighbors, but is restricted by the requirement of unitary dynamics. In addition, the no-cloning rule outlaws parallel updating. The latter obstacle can be overcome by using at least two species of qubits and updating each species separately [5]. In this work we assume two-level quantum cells, referred to as qubits. In addition, we explore only radius one evolution, in which each qubit interacts only with its nearest neighbors.

Given that CCA are valuable in the simulation of complex classical systems, it is natural to ask whether a QCA could be used to simulate complex quantum systems. Of course, a QCA that is universal can simulate any dynamics. The question is whether the unique architecture of the QCA can provide a less taxing experimental venue or provide further insight into complex dynamics. As a first step towards answering these questions, we explore the ability of a QCA to implement random unitary operators efficiently.

Random matrices were introduced by Wigner to describe the energy levels of atomic nuclei [7]. Since then, random matrices have been used as statistical models for a host of complex systems in many areas of physics [8]. From a quantum computation standpoint, some of the important systems modeled via random matrices include quantum systems whose classical dynamics are chaotic [9], decoherence [10], and quantum computer error models [11]. Thus, the ability to implement a random unitary operator allows for the simulation and study of these types of systems.

Beyond simulations, random unitary operators and random quantum states, created by applying a random

---

\*To whom correspondence should be addressed; Electronic address: weinstei@dave.nrl.navy.mil

†Electronic address: hellberg@dave.nrl.navy.mil

unitary to a computational basis state, play a vital role in quantum communication and computation. In quantum communication, random states are known to saturate the classical communication capacity of a noisy quantum channel [12]. In addition, superdense coding of quantum states [13], a reduction in key length for approximate encryption of quantum states, and the construction of more efficient data hiding schemes are protocols enabled by random unitary operators [14]. Random unitaries can also decrease the classical communication cost for remote state preparation [15]. Quantum computing protocols facilitated by random unitaries include quantum process tomography via a fidelity decay experiment using a random operator. Since random unitaries will not commute with noise sources effecting the system, they can identify the type and strength of the noise [16]. Random quantum states can be used for unbiased sampling, and the amount of multi-partite entanglement in random states approaches the maximum at a rate exponential with the number of qubits in the system [17].

The appropriate measure against which random unitary operators and quantum states are defined is the Haar measure on the group  $U(N)$ , where  $N$  is the dimension of Hilbert space. The random ensemble of unitaries drawn from this measure is the circular unitary ensemble (CUE) [18]. Unfortunately, an exact parameterization of CUE via the Hurwitz decomposition [19] requires exponential computing resources. Recently, however, pseudo-random unitary operators were introduced as efficiently implementable substitutes that fulfill various criteria of randomness and can be used in the above mentioned protocols [16].

The algorithm to produce pseudo-random operators, or maps, consists of  $m$  iterations of the  $n$  qubit gate: apply a random  $SU(2)$  rotation on each qubit, then evolve the system via all nearest neighbor couplings [16]. A random  $SU(2)$  rotation on qubit  $j$  during iteration  $i$  is defined as

$$R(\theta_i^j, \phi_i^j, \psi_i^j) = \begin{pmatrix} e^{i\phi_i^j} \cos \theta_i^j & e^{i\psi_i^j} \sin \theta_i^j \\ -e^{-i\psi_i^j} \sin \theta_i^j & e^{-i\phi_i^j} \cos \theta_i^j \end{pmatrix}, \quad (1)$$

and the nearest neighbor coupling operator is

$$U_{nnc} = e^{i(\pi/4)} \sum_{j=1}^{n-1} \sigma_z^j \otimes \sigma_z^{j+1}, \quad (2)$$

where  $\sigma_z^j$  is the  $z$ -direction Pauli spin operator. The random rotations are different for each qubit and each iteration, but the coupling is always  $\pi/4$  to maximize entanglement. After the  $m$  iterations, a final set of random rotations is applied.

This paper suggests a modified version of the above algorithm that can generate pseudo-random maps applicable to a QCA. The ability to efficiently generate such operators indicates that complex systems can be modeled and explored on a QCA. Moreover, the number of

iterations needed to create the pseudo-random operators for QCA is comparable the number needed for algorithms using a circuit model architecture.

The modification of the algorithm for application to a QCA system is straightforward. For each iteration, apply species specific random rotations followed by nearest neighbor coupling. Thus, iteration  $i$  of a QCA random map consists of applying random rotation  $U_i^A$  on all qubits of species  $A$ , followed by a different random rotation,  $U_i^B$ , applied to all qubits of species  $B$ , and so on for all  $k$  species of qubits, followed by  $U_{nnc}$ , given in equation 2. In keeping with the original algorithm a final rotation of the qubits is always applied.

This work may be viewed from a different perspective: an examination of how difficult (or easy) it is to create pseudo-random operators. The algorithm of [16] requires  $(3mn + 1)$  independent variables for a pseudo-random operator. Three independent variables per iteration for each random rotation, and one more for the coupling constants. However, as noted in [16], any universal gate set, no matter how biased, asymptotically generates the uniform measure of unitary operators. This does not imply that a universal gate set will efficiently generate the uniform measure of unitary operators. Nor does it suggest that a non-universal gate set cannot display some characteristics of randomness. Here, we attempt to reduce the number of independent variables required for the pseudo-random operator algorithm and see if it is still possible to efficiently generate CUE-like statistics. If not, we explore whether the generated operators demonstrate any characteristics of randomness. The modified pseudo-random operator algorithm for QCA requires only  $3mk + 1$  independent variables. Other possible ways of reducing the number of independent variables will also be discussed.

It is important to state that reducing the number of independent variable does not necessarily reduce the experimental difficulty in realizing the algorithm. Rather, experimental realizations would tend not to exhibit the symmetries that arise by reducing the number of independent variables as this would require acute precision over the internal and external system Hamiltonians. In this work, the first attempts at randomness are always via operators with maximum symmetries as these are the most difficult cases with which to achieve randomness.

Throughout this paper we avoid specifying the actual quantum computing hardware beyond the assertion of a  $\sigma_z^j \sigma_z^{j+1}$  coupling between nearest neighbor qubits. The  $\sigma_z^j \sigma_z^{j+1}$  interaction is used in the original pseudo-random operator algorithm and is appropriate for certain proposed realizations of quantum information processing. Systems such as quantum dots, however, interact via the Heisenberg interaction,  $\hat{\mathbf{S}}^j \cdot \hat{\mathbf{S}}^{j+1}$ , which has a total spin symmetry. Rotating all the qubits in parallel, as done for the  $k = 1$  QCA, commutes with the Heisenberg interaction and no randomness will be generated. This symmetry can be broken and random statistics regained

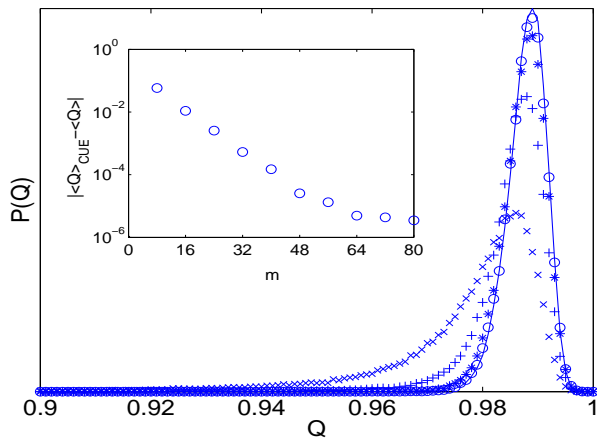


FIG. 1: Distribution of the multi-partite entanglement,  $Q$ , for  $m = 16$  (x), 24, (+), 32 (\*), and 40 (o) compared to the distribution of  $Q$  for CUE random operators (solid line).  $Q$  is calculated for the wavefunctions produced from evolving all (256) possible computational basis states under each of 500 eight-qubit maps for each  $m$  value. For  $m = 40$  the distribution is barely distinguishable from the CUE distribution. These distributions are similar to those found in [16] despite the further constraints imposed by the QCA architecture. The inset shows the difference between the average  $Q$  of states from the QCA operators and operators drawn from CUE as a function of  $m$ .

with a two-species QCA. Moreover, the spin-orbit coupling present in actual quantum dots, generally considered a negative and worthy of cancellation[20], introduces anisotropy into the system, breaking the symmetry and allowing for randomness even with the  $k = 1$  QCA.

The introduction of different random rotations at each iteration is not in accordance with typical CCA evolution, which follows the same rule at each time step. Nonetheless, the advantages of the QCA architecture, namely the reduced need of external Hamiltonian localization and control requirements, are still manifest in this algorithm.

The first QCA we explore is a single  $k = 1$  species chain. Every qubit in the chain rotates in parallel at every iteration. This map requires only  $3m + 1$  independent variables and has an inherent mirror symmetry stemming from the equivalence of evolution for all qubits barring those at the edges of the chain. Perhaps surprising is that, despite the simplicity of the system and the inherent mirror symmetry of the operators, the operators fulfill several statistical measures of randomness.

As mentioned above, the production of entanglement is one of the motivations for implementing random unitary operations. Figure (1) shows the distribution of  $Q$ , the multi-partite entanglement measure [21, 22], for states produced from QCA maps operating on computational basis states:

$$Q = 2 - \frac{2}{n} \sum_{j=1}^n \text{Tr}[\rho_j^2], \quad (3)$$

where  $\rho_j$  is the reduced density matrix of qubit  $j$ . As  $m$ , the number of iterations, increases, the distribution approaches that of CUE operators acting on the same states. For  $m = 40$  the distribution of  $Q$  is practically indistinguishable from that of CUE [17]. This is the same value of  $m$  necessary for the circuit model pseudo-random operator algorithm to produce a similar distribution.

Though the maps generated for the QCA,  $k = 1$  architecture follow the CUE entanglement distribution, they deviate from the expected random statistics for other important distributions. Perhaps the most widely used statistic for the randomness of operators are the spacings between nearest neighbor eigenvalues (or in the case of unitary matrices, eigenangles). For matrices of the CUE the expected distribution is [18]:

$$P_{CUE}(s) = \frac{32s^2}{\pi^2} e^{4s^2/\pi}. \quad (4)$$

where  $s$  is the difference between two ordered eigenvalues. The mirror symmetry of the system insures that the operator eigenvalues will not follow this distribution. Rather, the statistics follow the superposition of two independent CUE spectra, as shown in figure (2). The total distribution for a matrix of two unequal size blocks both with CUE distribution, derived from [23], is

$$\begin{aligned} P_{CUE}^{(2)}(s, g_1, g_2) &= 2g_1g_2[1 - \text{erf}_1 - \text{erf}_2 + \text{erf}_1\text{erf}_2] \\ &+ \frac{32}{\pi^2} s^2 e^{-4(g_1^2 + g_2^2)s^2/\pi} (g_1^4 + g_1^2g_2^2 + g_2^4) \\ &+ \frac{8}{\pi} g_1g_2s \left[ g_1 e^{-4g_1^2s^2/\pi} (1 - g_1^2 \frac{4s^2}{\pi}) \text{erfc}_2 \right. \\ &\left. + g_2 e^{-4g_2^2s^2/\pi} (1 - g_2^2 \frac{4s^2}{\pi}) \text{erfc}_1 \right], \quad (5) \end{aligned}$$

where  $g_i$  is the fraction of Hilbert space spanned by block  $i = 1, 2$ , and  $\text{erf}_i = \text{erf}(\frac{2g_i s}{\sqrt{\pi}})$  and  $\text{erfc}_i = \text{erfc}(\frac{2g_i s}{\sqrt{\pi}})$  are the error function and complementary error function respectively. For an 8 qubit operator with mirror symmetry,  $g_1 = 15/32$ ,  $g_2 = 17/32$ , and the resulting distribution is barely distinguishable from the  $g_1 = g_2 = 1/2$  case,

$$\begin{aligned} P_{CUE}^{(2)}(s) &= \frac{1}{2} \text{erfc}(\frac{s}{\sqrt{\pi}})^2 + \frac{6}{\pi^2} s^2 e^{-2s^2/\pi} \\ &+ \frac{2}{\pi} s e^{-s^2/\pi} (1 - \frac{s^2}{\pi}) \text{erfc}(\frac{s}{\sqrt{\pi}}). \quad (6) \end{aligned}$$

The elements of the eigenvectors of random operators also follow ensemble specific distributions. For CUE the appropriate distribution, as  $N \rightarrow \infty$ , is [18]:

$$P_{CUE}(y) = e^{-y} \quad (7)$$

where  $y = N\eta$ , and  $\eta$  is the squared modulus of the eigenvector element. The randomness of the eigenvector elements determines the systems response to perturbation in the sense of fidelity decay [24]. The eigenvector

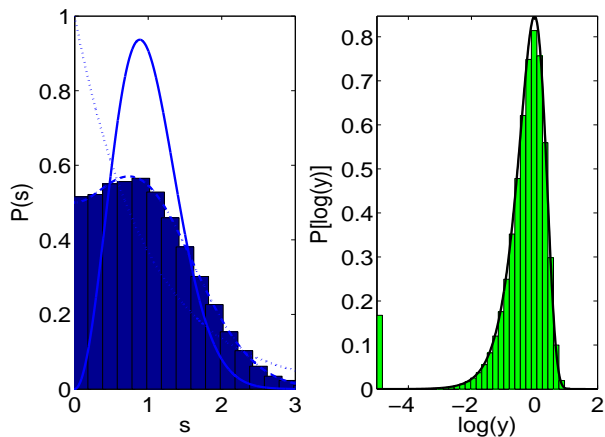


FIG. 2: Statistical measures of randomness for 100 one-species,  $m = 40$ , eight-qubit QCA maps. The left figure shows the distribution of  $s$ , the nearest neighbor eigenangle spacings compared to that expected for random unitary operators (solid line), regular integrable operators (dotted line), and a CUE operator with mirror symmetry (dash-dot line). The distribution follows that expected for a random operator with mirror symmetry. The right figure shows the distribution of the magnitude of the eigenvector elements  $y$  compared to the distribution expected from CUE. There is a noticeable deviation from the random distribution. This is seen most clearly by the large number of very small terms,  $y < 10^{-5}$ , depicted by the spike at the left of the figure. Nevertheless, the fidelity decay behavior of the maps (not shown), which depends on the eigenvector statistics, follows the expected exponential of random maps.

element distribution of  $k = 1$  QCA maps deviate slightly from the CUE distribution, as seen in figure (2). Nevertheless, these maps demonstrate the exponential decay of fidelity at the rate expected for CUE operators.

To summarize, while these operators are not random with respect to the Haar measure, they appear sufficiently random for entanglement production. They may also be used for protocols relying on randomness of eigenvectors such as random operator quantum process tomography [16] (for noise that does not have the symmetry of the maps) and for modeling complex quantum dynamics that have inherent symmetries.

The failure of the above operators to fulfill certain criteria of randomness can be rectified by breaking the mirror symmetry of the system. We provide two examples. The first is by having a two species QCA chain  $ABAB \dots$  with an even number of qubits. For this  $k = 2$  map, iteration  $i$  of the circuit consists of a random  $SU(2)$  rotation  $U_i^A$  on all qubits of species  $A$ , followed by a random  $SU(2)$  rotation  $U_i^B$  applied to all qubits of species  $B$ , followed by coupling between nearest neighbor qubits,  $U_{nnc}$ . Thus, the number of independent variables for the generated operator is  $6m$  for the two random rotations per iteration plus one more for the coupling. As shown in figures (3) and (4) all of the tested criteria of randomness are

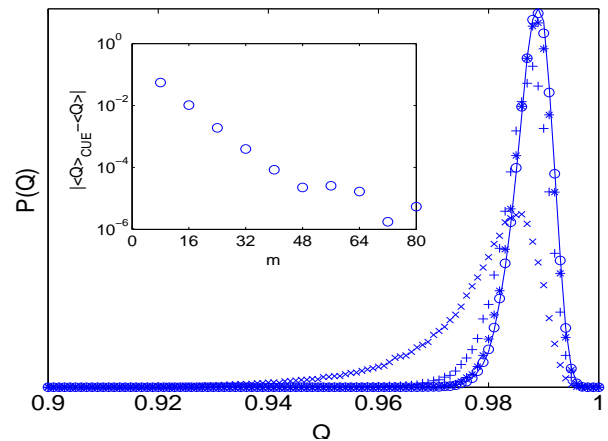


FIG. 3: Distribution of the multi-partite entanglement,  $Q$ , for two-species QCA maps of  $m = 16$  (x), 24, (+), 32 (\*), and 40 (o) compared to the distribution for CUE random operators. As in the case of a one species QCA, the  $m = 40$  distribution is barely distinguishable from the CUE distribution, despite the constraints imposed by the QCA architecture. The inset shows the difference between the average  $Q$  for states from the QCA and CUE operators as a function of  $m$ .

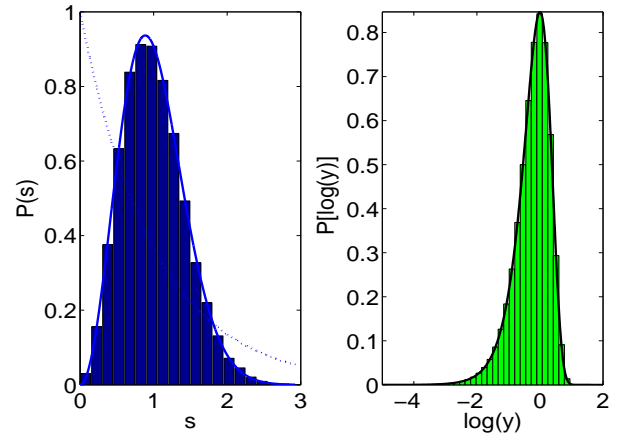


FIG. 4: Statistical measures of randomness for 100 two-species,  $m = 40$ , QCA maps. The left figure shows the distribution of  $s$  the nearest neighbor eigenangle spacings compared to that expected for CUE operators (solid line), and regular integrable maps (dotted line). The right figure shows the distribution of the magnitude of the eigenvector elements  $y$  compared to that expected for CUE (solid line). Both criteria of randomness are fulfilled by the  $k = 2$  map.

fulfilled for these maps.

A second way to break the mirror symmetry of the  $k = 1$  QCA is by changing the value of one of the nearest neighbor couplings (though not the center coupling). In this way the map requires only  $3m + 2$  independent variables while still fulfilling all of the above criteria of randomness. An operator generated from a system with unequal nearest neighbor couplings is especially relevant

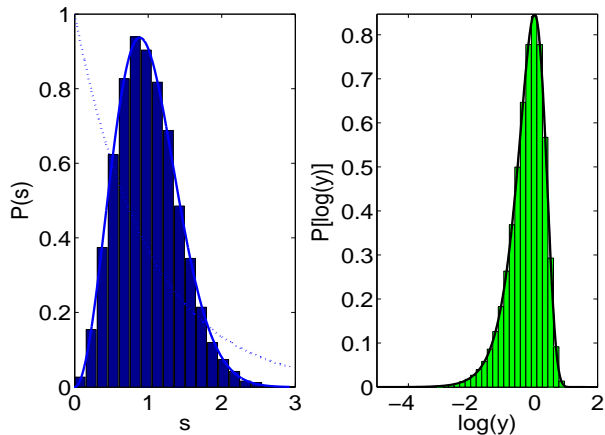


FIG. 5: Statistical measures of randomness for 100  $m = 40$ , one-species QCA rings. In this instance, all nearest neighbor couplings are equal to  $\pi/4$  except for two, one of which has a coupling of  $\pi/5$  and the other a coupling of  $\pi/4.5$ . The left figure shows the distribution of  $s$  the nearest neighbor eigenangle spacings compared to that expected for CUE operators (solid line) and regular integrable maps (dotted line). The right figure shows the distribution of the magnitude of the eigenvector elements  $y$  compared to the CUE distribution. QCA architecture with unequal nearest neighbor couplings (be it a ring or chain) are the most likely for experimental implementations.

for experimental implementations. For many quantum computer hardware proposals attaining exact equal couplings between qubits is nearly impossible. An actual chain of qubits, such as in nuclear magnetic resonance or quantum dots, could not be expected to have the mirror symmetry assumed above. As we have demonstrated, however, this allows such systems to more easily generate pseudo-random states and operators.

The discussion to this point has centered around QCA chains. If the QCA were structured as a ring (which, experimentally, may be more difficult) such that all qubits had two nearest neighbors, we have checked that the symmetries inherent in the system do not allow for enough entanglement production following the random distribution of  $Q$ , regardless of the number of iterations. However, if one of the couplings is (even slightly) different than the others the random distribution of  $Q$  is recovered as the system is then equivalent to the QCA chain. If two couplings are different (from the others and each other), all symmetries have been broken and full pseudo-randomness is recovered as shown in figure (5).

There are other ways to reduce the number of independent variables in the pseudo-random operator algorithm besides a QCA. We explore some of these possibilities in attempt to achieve aspects of randomness with as few independent variables as possible. First, we explore what is, in some sense, the opposite of the QCA discussed above. For the QCA operators the same rotation was applied to every qubit but the rotation was different for

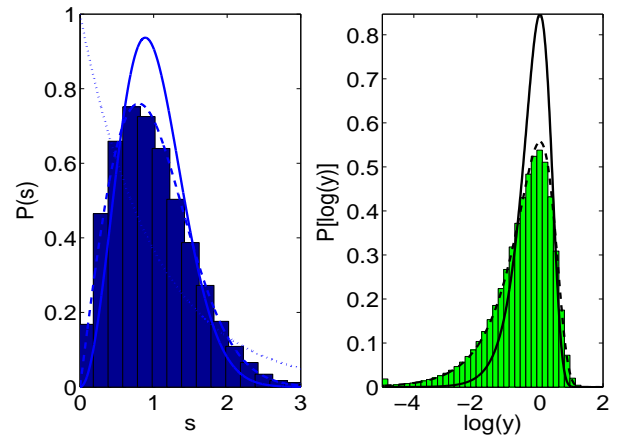


FIG. 6: Statistical measures of randomness for 100  $m = 40$ , repeat maps. The left figure shows the distribution of  $s$  the nearest neighbor eigenangle spacings compared to the expected distributions for CUE operators (solid line), regular integrable systems (dotted line) and COE operators (dashed line). The right figure shows the distribution of the magnitude of the eigenvector elements  $y$  compared to the CUE (solid line) and COE (dashed line) distributions. Both distributions are similar to those of the COE universal symmetry class.

each iteration. We now study operators in which a different random rotation is applied to each qubit but the rotation is the same at every iteration. As before there is a  $\pi/4$  nearest neighbor coupling evolution between the rotations. These operators, to which we shall refer to as repeat maps, require only  $3n + 1$  independent variables.

Given the structure of repeat maps, the repetition of the same operation over and over, it is clear that they have time-reversal invariance, applying the map backwards produces the same results as applying it forward. Hence, the eigenvalue and eigenvector statistics deviate only slightly from the distribution appropriate for random orthogonal matrices. The circular orthogonal ensemble (COE) includes unitary operators that have anti-unitary symmetry (time reversal invariance) and is a subset of the general CUE. The level spacing for the COE class is [18]:

$$P_{COE}(s) = \frac{\pi s}{2} e^{-\pi s^2/4}, \quad (8)$$

and the distribution of the elements of the eigenvectors of COE matrices as  $N \rightarrow \infty$  are [18]

$$P_{COE}(y) = \frac{1}{\sqrt{2\pi y}} e^{-y/2}. \quad (9)$$

The operators of many quantum analogs of classically chaotic systems belong to the COE class and, therefore, repeat maps may form appropriate models for these systems. However, repeat maps do not produce the entanglement distribution expected for random operators.

Finally, we turn to versions of the pseudo-random operator algorithm which faithfully follow the evolution of

CCA. As explained, there are two major characteristics of CCA evolution: homogeneity of evolution for each cell, and homogeneity of evolution at each time step. In the first part of this work, we examined evolution in accordance with only the first of these characteristics. Repeat maps describe evolution with only the second characteristic. Currently, we explore the dynamics of maps that evolve as CCA in both respects: each qubit rotates via the same random  $SU(2)$  rotation,  $U$ , and that rotation is the same for all iterations. This gives a total of only  $3 + 1$  independent variables for the entire operator.

As these QCA maps are even more limited than the repeat maps discussed above, it is no surprise that the entanglement produced by these maps do not follow the distribution of random maps. However, these maps deviate only slightly in the other criteria of randomness. As shown in figure (7) the eigenvector element distribution deviates somewhat from the COE distribution while the nearest-neighbor spacing distribution deviates only slightly from the global statistics expected from a map with two differently sized COE blocks due to mirror symmetry [23]

$$\begin{aligned}
P_{COE}^{(2)}(s, g_1, g_2) &= \frac{\pi}{2} s g_1^3 \operatorname{erfc} \left( \frac{\sqrt{\pi} g_2 s}{2} \right) e^{-\pi g_1^2 s^2 / 4} \\
&+ \frac{\pi}{2} s g_2^3 \operatorname{erfc} \left( \frac{\sqrt{\pi} g_1 s}{2} \right) e^{-\pi g_2^2 s^2 / 4} \\
&+ 2 g_1 g_2 e^{-\pi s^2 (g_1^2 + g_2^2) / 4}, \quad (10)
\end{aligned}$$

with  $g_1$  and  $g_2$  defined as above. As with the CUE mirror symmetry operator, the resulting distribution is barely distinguishable from the  $g_1 = g_2 = 1/2$  case

$$P_{COE}^{(2)}(s) = \frac{1}{2} \left( \operatorname{erfc} \left( \frac{\sqrt{\pi} s}{4} \right) \frac{\pi s}{4} e^{-\pi s^2 / 16} + e^{-\pi s^2 / 8} \right) \quad (11)$$

As with the QCA maps discussed at the beginning of this work, the mirror symmetry of the system can be broken by changing one of the couplings. In this way the eigenvalue and eigenvector statistics revert back to the COE distributions seen in the repeat map and shown in figure (8). This operator requires only  $3 + 2$  independent variables.

Perhaps it should come as no surprise that operators with so few independent variables can still fulfill criteria of randomness. Quantum chaos models, such as the quantum sawtooth and quantum Harper's map [25, 26], have only one or two free parameters, yet, fulfill criteria of randomness, and can be efficiently implemented on a quantum computer. What we have shown here, however, is that quantum chaos models are not exceptional cases, showing randomness due to their connection with a classically chaotic analog. Rather, most operators with few random variables will still show many characteristics of randomness. Regularity is the exception, randomness is the general rule.

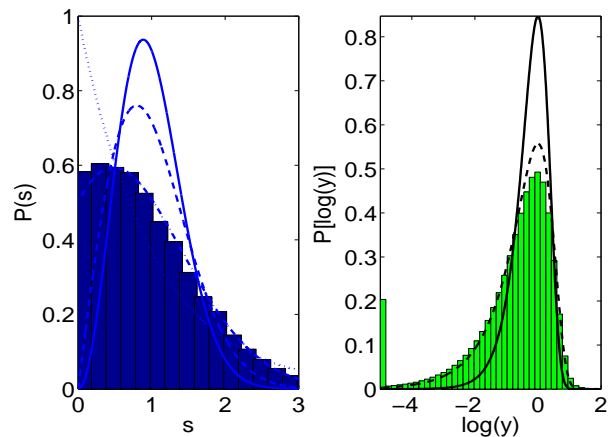


FIG. 7: Statistical measures of randomness for 100  $m = 40$ ,  $k = 1$ , QCA maps in which there is only one random rotation. This one rotation is applied to each qubit at each iteration. The left figure shows the distribution of  $s$  the nearest neighbor eigenangle spacings compared to the global spectral statistics of a COE operator with mirror symmetry (dash-dot line), and the right figure shows the distribution of the magnitude of the eigenvector elements  $y$ . Both distributions are similar to those of the COE universal symmetry class.

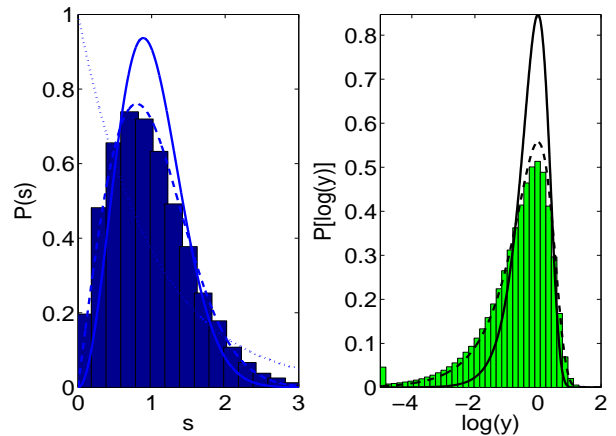


FIG. 8: Statistical measures of randomness for 100  $m = 40$ ,  $k = 1$ , QCA maps in which the same random rotation is applied to each qubit at each iteration. In these maps one of the nearest neighbor couplings in the chain is  $\pi/5$  while all the rest are  $\pi/4$ . The left figure shows the distribution of  $s$  the nearest neighbor eigenangle spacings compared to COE, and the right figure shows the distribution of the magnitude of the eigenvector elements  $y$  compared to that expected to COE.

In conclusion, we have demonstrated that general aspects of complex quantum dynamics can be studied on a QCA architecture. The evidence behind this supposition is the ability to generate pseudo-random operators that fulfill general criteria of randomness. These operators are appropriate substitutes for random operators which are often used as models of complex quantum systems and play an important role in other quantum infor-

mation processing protocols. Throughout this work we have attempted to introduce operators generated by as few independent variables as possible. These operators are tested to determine whether they meet the various criteria of randomness. Operators which do not fulfill all of the criteria may nevertheless prove useful in certain simulations of quantum systems and other quantum computational protocols. The minimum number of independent variables is reached via simulation of an algorithm which mimics classical cellular automata evolution. Yet, even these operators demonstrate many aspects of randomness. This implies that even with few independent variables most operators will tend towards randomness.

The authors would like to thank S. Montangero for helpful discussions. The authors acknowledge support from the DARPA QuIST (MIPR 02 N699-00) program. Y.S.W. acknowledges the support of the National Research Council Research Associateship Program through the Naval Research Laboratory. Computations were performed at the ASC DoD Major Shared Resource Center.

- 
- [1] D. Deutsch, Proc. R. Soc. Lond. A, **400**, 97, (1985).
  - [2] S. Lloyd, Science, **261**, 1569, (1993).
  - [3] J. Watrous, *Proceedings of the 36th IEEE Symposium on the Foundations of Computer Science*, 528, (1995).
  - [4] S.C. Benjamin, Phys. Rev. A, **61**, 020301, (2000).
  - [5] G.K. Brennen, J.E. Williams, Phys. Rev. A **68**, 042311 (2003).
  - [6] S. Wolfram, *A New Kind of Science*, (Wolfram Media, Champaign, 2002).
  - [7] E.P. Wigner, Ann. Math. **62**, 548 (1955); **65**, 203 (1957).
  - [8] See T. Guhr, A. Müller-Groeling, H.A. Weidenmüller, Phys. Rep., **299**, 189, (1998) for a comprehensive review.
  - [9] O. Bohigas, M.J. Giannoni, C. Schmit, Phys. Rev. Lett., **52**, 1, (1984); F. Haake, *Quantum Signatures of Chaos*, (Springer, New York, 1992).
  - [10] T. Gorin, T.H. Seligman, J. Opt. B, **4**, 386, (2002).
  - [11] T. Prosen, M. Znidaric, J. Phys. A, **34**, L681, (2001).
  - [12] S. Lloyd, Phys. Rev. A, **55**, 1613, (1997).
  - [13] A. Harrow, P. Hayden, D. Leung, quant-ph/0307221.
  - [14] P. Hayden, D. Leung, P. Shor, A. Winter, quant-ph/0307104.
  - [15] C.H. Bennett, P. Hayden, D. Leung, P. Shor, A. Winter, quant-ph/0307100.
  - [16] J. Emerson, Y.S. Weinstein, M. Saraceno, S. Lloyd, D.G. Cory, Science, **302**, 2098, (2003).
  - [17] A. Scott, C. Caves, J. Phys. A, **36**, 9553, (2003).
  - [18] M.L. Mehta, *Random Matrices*, (Academic Press, New York, 1991).
  - [19] M. Pozniak, K. Zyczkowski, M. Kus, J. Phys. A, **31**, 1059, (1998).
  - [20] N.E. Bonesteel, D. Stepanenko, D.P. DiVincenzo, Phys. Rev. Lett., **87**, 207901, (2001); G. Burkard, D. Loss, Phys. Rev. Lett., **88**, 047903, (2002).
  - [21] D.A. Meyer, N.R. Wallach, J. Math. Phys., **43**, 4273, (2002).
  - [22] G.K. Brennen, Quant. Inf. Comp., **3**, 619, (2003).
  - [23] N. Rosensweig, C.E. Porter, Phys. Rev., **120**, 1698, (1960); O. Bohigas, *Les Houches Lecture Series*, edited by M.J. Giannoni, A. Voros, J. Zinn-Justin, (North-Holland, Amsterdam, 1991), Vol. 52.
  - [24] J. Emerson, Y.S. Weinstein, S. Lloyd, D.G. Cory, Phys. Rev. Lett., **89**, 284102, (2002).
  - [25] F. Haake, M. Kus, R. Scharf, Z. Phys. B, **65**, 381 (1987).
  - [26] P. Leboeuf, J. Kurchan, M. Feingold, D.P. Arovas, Phys. Rev. Lett. **65**, 3076, (1990).